

Ultrasonically Induced Polymerization and Polymer Grafting in the Presence of Carbonaceous Nanoparticles

Authors:

Sarah Cohen, Evgeni Zelikman, Ran Yosef Suckeveriene

Date Submitted: 2021-07-29

Keywords: polymerization, grafting, nanoparticles, sonochemistry

Abstract:

Nanotechnology refers to technologies using at least one nanometric dimension. Most advances have been in the field of nanomaterials used in research and industry. The vast potential of polymeric nanocomposites for advanced materials and applications such as hybrid nanocomposites with customized electrical conductivity, anti-bacterial, anti-viral, and anti-fog properties have attracted considerable attention. The number of studies on the preparation of nanocomposites in the presence of carbon materials, i.e., carbon nanotubes (CNTs) and graphene, has intensified over the last decade with the growing interest in their outstanding synergic properties. However, the functionality of such nanocomposites depends on overcoming three key challenges: (a) the breakdown of nanoparticle agglomerates; (b) the attachment of functional materials to the nanoparticle surfaces; and (c) the fine dispersion of functional nanoparticles within the polymeric matrices. Ultrasonic polymerization and grafting in the presence of nanoparticles is an innovative solution that can meet these three challenges simultaneously. These chemical reactions are less well known and only a few research groups have dealt with them to date. This review focuses on two main pathways to the design of ultrasonically induced carbon-based nanocomposites: the covalent approach which is based on the chemical interactions between the carbon fillers and the matrix, and the non-covalent approach which is based on the physical interactions.

Record Type: Published Article

Submitted To: LAPSE (Living Archive for Process Systems Engineering)

Citation (overall record, always the latest version):

LAPSE:2021.0686

Citation (this specific file, latest version):

LAPSE:2021.0686-1

Citation (this specific file, this version):

LAPSE:2021.0686-1v1

DOI of Published Version: <https://doi.org/10.3390/pr8121680>

License: Creative Commons Attribution 4.0 International (CC BY 4.0)

Review

Ultrasonically Induced Polymerization and Polymer Grafting in the Presence of Carbonaceous Nanoparticles

Sarah Cohen ¹, Evgeni Zelikman ² and Ran Yosef Suckeveriene ^{1,*}

¹ Water Industries Engineering, Kinneret Academic College, Zemach 1513200, Israel; sarah.cohen00000@gmail.com

² Tosaf, Additive and White Division, R&D, Afula 1812601, Israel; zjenia@gmail.com

* Correspondence: ransots@mx.kinneret.ac.il or ransots@gmail.com; Tel.: +972-54-9985425

Received: 26 August 2020; Accepted: 17 December 2020; Published: 19 December 2020



Abstract: Nanotechnology refers to technologies using at least one nanometric dimension. Most advances have been in the field of nanomaterials used in research and industry. The vast potential of polymeric nanocomposites for advanced materials and applications such as hybrid nanocomposites with customized electrical conductivity, anti-bacterial, anti-viral, and anti-fog properties have attracted considerable attention. The number of studies on the preparation of nanocomposites in the presence of carbon materials, i.e., carbon nanotubes (CNTs) and graphene, has intensified over the last decade with the growing interest in their outstanding synergic properties. However, the functionality of such nanocomposites depends on overcoming three key challenges: (a) the breakdown of nanoparticle agglomerates; (b) the attachment of functional materials to the nanoparticle surfaces; and (c) the fine dispersion of functional nanoparticles within the polymeric matrices. Ultrasonic polymerization and grafting in the presence of nanoparticles is an innovative solution that can meet these three challenges simultaneously. These chemical reactions are less well known and only a few research groups have dealt with them to date. This review focuses on two main pathways to the design of ultrasonically induced carbon-based nanocomposites: the covalent approach which is based on the chemical interactions between the carbon fillers and the matrix, and the non-covalent approach which is based on the physical interactions.

Keywords: sonochemistry; grafting; nanoparticles; polymerization

1. Introduction

1.1. Carbon-Based Materials

Carbon nanomaterials are classified as zero-dimensional (fullerene), one-dimensional (carbon nanotubes, CNTs) or two-dimensional (graphene). The main advantages of CNTs (their high stiffness, flexibility and tensile strength, along with their thermal and electrical conductivity) and graphene (which has extraordinary mechanical, electronic, and conductive properties coupled with a high surface area) make them highly promising for a wide range of applications from energy storage to optoelectronics to biomedical devices. Many of the distinctive properties of carbon nanomaterials derive from the fact that all carbon nanomaterials are made of sp^2 hybridized carbon [1].

These carbon-based materials have attracted considerable interest as potential nanofillers for the fabrication of carbon-based nanocomposites. However, their prime drawback is their tendency to agglomerate, which makes them much less effective in nanocomposites [2]. Several methods have been put forward to achieve good, stable dispersion. One such technique is ultrasonically assisted polymerization in the presence of nanoparticles [3–7].

1.2. Ultrasonication

Richards et al. [8] were the first to report the use of ultrasound to improve chemical reactions. Ultrasound waves are produced in the frequency range of 20 kHz to 500 MHz. Ultrasonication involves applying high shear force while mixing. The mechanism of sonication relies on a phenomenon known as cavitation where ultrasonic waves create bubbles within a medium which grows until it collapses violently under the influence of high- and low-pressure waves [9,10].

Ultrasonication makes it possible to work at low temperature and pressure in a one-pot process while achieving high yield and reaction rates. However, several parameters affect cavitation: (a) the reaction temperature, (b) the solvent and (c) the ultrasonic frequency and intensity [9,11], among others. In the laboratory, ultrasonication is produced by an ultrasonic probe [12–14].

1.3. Interfacial Interactions Between the Fillers and the Matrix

High quality -nanocomposites require the uniform dispersion of carbon fillers within the polymeric matrix which can be achieved by strong interfacial contact between the inorganic fillers and the organic polymer and high nanofiller loading [15]. Espinosa-González et al. [12] showed that polystyrene (PS)/multi-wall carbon nanotube (MWCNT) nanocomposites with an 80%-CNT content resulted in a very inhomogeneous coating. By contrast, lowering the CNT content by a factor of two resulted in uniform grafting of the PS onto the CNT surface, where ~40% of the CNT content remained high. Thus, differences in filler content have a real impact on good carbon nanomaterial dispersion within the matrix.

High surface contact within polymer composites filled with carbon nanomaterials can be achieved by employing both non-covalent and covalent approaches. To obtain covalent linkages, the most common method is grafting and in particular the “grafting-from” approach. The main technique for producing non-covalent polymer and carbon bonding is known as in situ polymerization. These two approaches are discussed separately below.

2. Covalent Interactions

Extensive research has centered on in situ polymerization for the preparation of the composites within which the polymer is grafted to the nanocarbon surface. The advantage of creating covalent bonding between the carbon fillers and the matrix is related to the ability of the control filler loading to obtain ordered nanocarbons while still obtaining good dispersion of the carbon fillers into the matrix. There are several different grafting approaches, including the popular “grafting-from” approach. Numerous studies have examined grafting-from polymerization when the polymer is covalently attached to the surface of carbon-based materials and grows on the surface of the tubes or graphene. However, only a few have investigated grafting-from under sonication. Monomers can be grown using different types of polymerization including reversible-addition-fragmentation chain transfer polymerization (RAFT), ring-opening polymerization (ROP), atom transfer radical polymerization (ATRP), and inverse emulsion polymerization [16–18].

2.1. CNT-Based Nanocomposites

2.1.1. Grafting-from through Surface-Initiated Polymerization

The “grafting-from” polymerization approach can produce a core-shell structure nanocomposite. This method can be used to build optoelectronic devices where obtaining an ordered interface between CNTs and the conjugated polymer is particularly hard to design but constitutes a precondition for its efficiency. Surface-initiated polymerization is the most common way to fabricate core-shell structures. The key to this process is the covalent immobilization of the initiator of the CNTs [19]. When the monomers are introduced, they can therefore grow directly from the CNT surfaces to form these structures.

Hou et al. [20] carried out a surface-initiated Kumada catalyst-transfer polycondensation (SI-KCTP) of the monomer 2-bromo-5-chloromagnesio-3-hexylthiophene in the presence of the initiator 1,2-bis(diphenylphosphino)propane (DPPP) and multi-wall carbon nanotubes (MWCNTs), resulting in the formation of MWCNT-g-P3HT nanocomposites in which well-defined chains of poly(3-hexylthiophene) (P3HT) grew from the surfaces of MWCNT while maintaining ordered heterojunctions. As seen in Figure 1, the grafting-from polymerization yielded a core-shell structure in which cylinder-shaped heterojunctions were formed leading to highly-ordered P3HT aggregates. The SI-KCTP enabled the formation of regioregular P3HT (as demonstrated by the observation of a peak in the nuclear magnetic resonance (NMR) spectroscopy attributed to the head- to- tail arrangement of the P3HT repeat units) which could be harnessed to control the polymer chain lengths (the linear increase in the grafted P3HT as a function of the monomer to initiator). The nanocomposites also displayed red-shifted and well-resolved absorption maxima, thus confirming the formation of highly ordered aggregates covalently attached to the surface of the MWCNT. The key step was found to be the anchoring of the initiator DPPP on the surface of the MWCNTs, because accurate control over the initial monomer to initiator ratio during the polymerization made it possible to adjust the length of the polymer chain length.

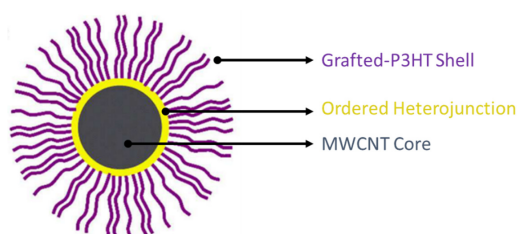


Figure 1. Core-shell structure of multi-walled carbon nanotube-g-poly(3-hexylthiophene) (MWCNT-g-P3HT) nanocomposites prepared by the “grafting-from” method (Reprinted (adapted) with permission from Hou, W.; Zhao, N.-J.; Meng, D.; Tang, J.; Zeng, Y.; Wu, Y.; Weng, Y.; Cheng, C.; Xu, X.; Li, Y.; et al. Controlled Growth of Well-Defined Conjugated Polymers from the Surfaces of Multiwalled Carbon Nanotubes: Photoresponse Enhancement via Charge Separation. *ACS Nano* **2016**, *10*, 5189–5198 [20]. Copyright (2020) American Chemical Society.).

The photoresponse capabilities of MWCNT-g-P3HT were evaluated by charge separation under illumination. Hou et al., reported that the core-shell structure acted efficiently as a donor/acceptor system because a photoinduced electron transfer was detected from the lowest unoccupied molecular orbital (LUMO) of the P3HT (electron donor) to the Fermi level (E_F) of the MWCNTs (electron acceptor) (Figure 2). They suggested that this was based on a two-step mechanism; namely, the rapid diffusion of the excitons in highly ordered P3HT layers followed by a dissociation of these excitons within the heterojunctions between the MWCNTs and P3HT.

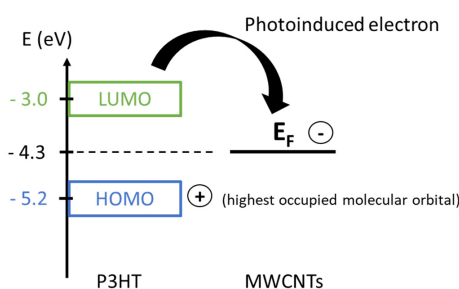


Figure 2. Energy-band diagrams of P3HT and MWCNTs (Reprinted (adapted) with permission from Hou, W.; Zhao, N.-J.; Meng, D.; Tang, J.; Zeng, Y.; Wu, Y.; Weng, Y.; Cheng, C.; Xu, X.; Li, Y.; et al. Controlled Growth of Well-Defined Conjugated Polymers from the Surfaces of Multiwalled Carbon Nanotubes: Photoresponse Enhancement via Charge Separation. *ACS Nano* **2016**, *10*, 5189–5198 [20]. Copyright (2020) American Chemical Society.).

In another study, MWCNTs were functionalized by brominated groups from the initiator 2-hydroxyethyl bromoisobutyrate (HEBB) under acidic treatment assisted by ultrasonication [5]. The surface-initiated atom transfer radical polymerization (SI-ATRP) of the monomer, 2,2,6,6-tetramethylpiperidin-4-yl methacrylate (TMPM) in the presence of the acidic-treated MWCNTs (MWCNT-initiator) took place at 60 °C for 16 h, followed by chemical oxidation resulting in MWCNT-g-poly(2,2,6,6-tetramethylpiperidin-1-oxyl-4-yl methacrylate) (PTMA) (MWCNT-g-PTMA). The main steps to producing MWCNT-g-PTMA can be seen in Figure 3. The thermogravimetric analysis (TGA) results confirmed the presence of initiator groups (the brominated groups were confirmed by X-ray photoelectron spectroscopy, XPS) on the surface of the nanotubes by a weight loss of 10% in the MWCNT-initiator. One of the main advantages of the SI-ATRP technique combined with the grafting-from method is the higher polymer grafting density on the MWCNTs [19].

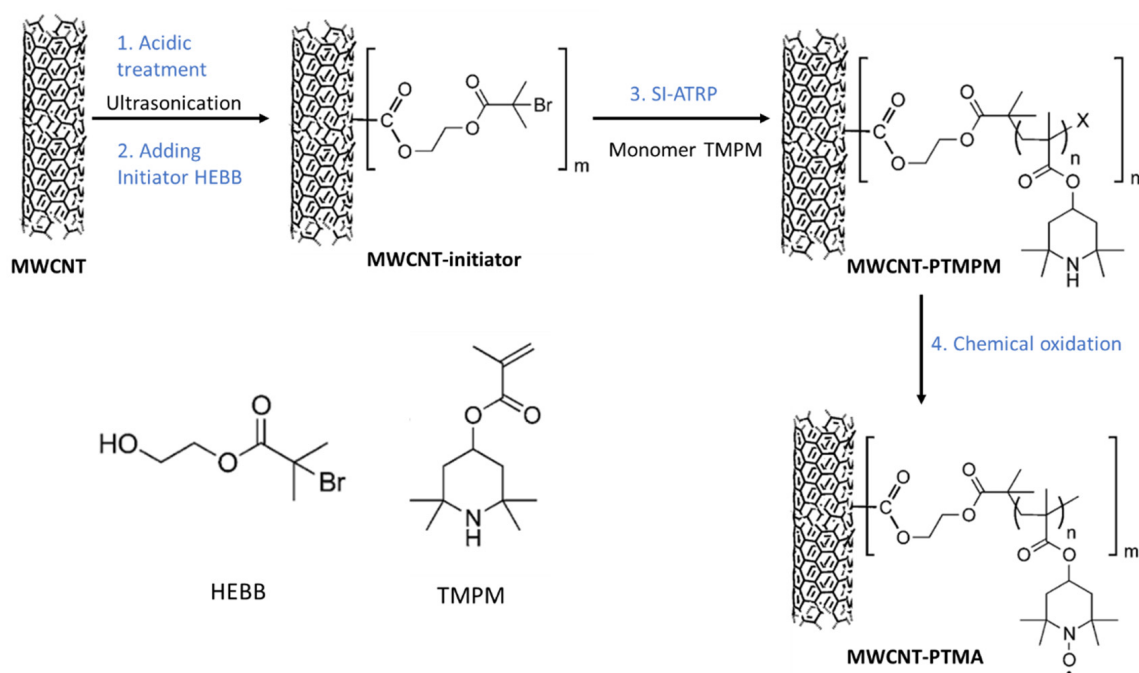


Figure 3. Preparation of poly(2,2,6,6-tetramethylpiperidin-1-oxyl-4-yl methacrylate) (PTMA) covalently grafted from MWCNTs by grafting-from polymerization (Republished with permission (2020) of the Royal Society of Chemistry from Ernould, B.; Devos, M.; Bourgeois, J.-P.; Rolland, J.; Vlad, A.; Gohy, J.-F. Grafting of a Redox Polymer onto Carbon Nanotubes for High Capacity Battery Materials. *J. Mater. Chem. A*. **2015**, *3*, 8832–8839 [5]. Permission conveyed through Copyright Clearance Center Inc.).

To characterize this structure, a series of tests were performed on the MWCNT-g-poly(2,2,6,6-tetramethyl-4-piperidyl methacrylate) (PTMPM) (MWCNT-g-PTMPM). Transmission electron microscopy (TEM) images (Figure 4) revealed the formation of a core-shell structure. The MWCNT-g-PTMPM diameter was greater than the neat MWCNTs (17 nm and 11 nm respectively), which confirmed the presence of an organic layer (shell) wrapping the MWCNTs (core). Moreover, the PTMPM covering was found to be uniform: the XPS graph of MWCNT-g-PTMPM was similar to the neat PTMPM but different from the MWCNT-initiator (a shoulder was not present). After the oxidation step converting MWCNT-g-PTMPM to MWCNT-g-PTMA, the core-shell structure remained, as well as the thermal properties. Ernould et al., also successfully proved that the MWCNT-g-PTMPM was an efficient cathodic electrode by showing that it presents both high cycling stability (87% of the initial capacity retention maintained after 200 charge/discharge cycles) and good specific capacity (85% of the theoretical capacity).

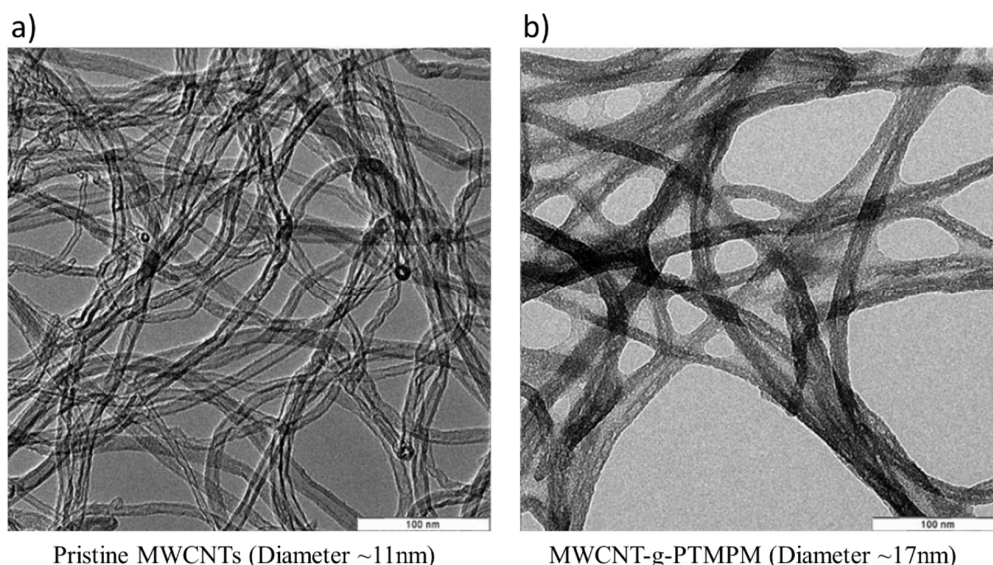


Figure 4. Transmission electron microscopy (TEM) micrographs of (a) pristine MWCNTs and (b) MWCNT-g-poly(2,2,6,6-tetramethyl-4-piperidyl methacrylate) (PTMPM) (MWCNT-g-PTMPM)—Scale bars: 100 nm (Republished with permission (2020) of the Royal Society of Chemistry from Ernould, B.; Devos, M.; Bourgeois, J.-P.; Rolland, J.; Vlad, A.; Gohy, J.-F. Grafting of a Redox Polymer onto Carbon Nanotubes for High Capacity Battery Materials. *J. Mater. Chem. A*. **2015**, *3*, 8832–8839 [5]. Permission conveyed through Copyright Clearance Center Inc.).

Yao et al. [21] discussed the challenges related to the dispersibility of acrylate-based polymer/single-walled carbon nanotube (SWCNT) nanocomposites within different organic solvents such as tetrahydrofuran (THF), acetone, or *N,N*-dimethylformamide (DMF). They showed that methyl methacrylate (MMA)/SWCNT composites were not soluble, but by replacing the former monomer by tert-butyl acrylate (tBuA), the nanocomposite's solubility was clearly enhanced. These two composites were synthesized by the same method: a “grafting-from” ATRP polymerization of the monomers initiated by alkyl bromide-based chain transfer agents (CTAs) grafted onto the CNT surfaces prior to the growth-chain polymerization, assisted by sonication. This resulted in a covalent attachment of the polymers onto the sidewalls of the CNTs. The authors showed that this solubility difference was due to the appearance of crosslinking reactions between the two chain ends of the MMA polymers derived either from a single CNTs or two different nanotubes.

In this study, Che et al. [22] greatly enhanced the dispersibility of aligned SWCNTs within the epoxy (EP) matrix by grafting-from a dendritic poly(amidoamine) (PAMAM) onto the CNT surface. The prior acidic-treated and isocyanate group-functionalized SWCNTs underwent a two-step reaction performed twice successively under sonication to achieve a four-branched dendrimer. This involved the formation of amino groups via the amidation reaction by the ethylenediamine (EDA) then conversion into ester groups by the addition of methyl acrylate. The authors showed that the grafting of dendrimer polymer to CNTs was key to achieving a uniform dispersion because without it, several micro-sized CNTs clusters formed in the EP matrix (Figure 5A) preventing suitable homogeneity of the SWCNTs. In addition, the increase in the branching degree of dendrimer enhances the solubility of the PAMAM/SWCNT nanocomposites in the epoxy matrix, given the higher number of amino groups which are likely to react with the matrix, as shown in Figure 5B,C. The longitudinal alignment of the SWCNTs created by spinning (Figure 5D) also contributed to the good dispersibility of the CNTs within the polymeric matrix, thus enhancing its mechanical properties.

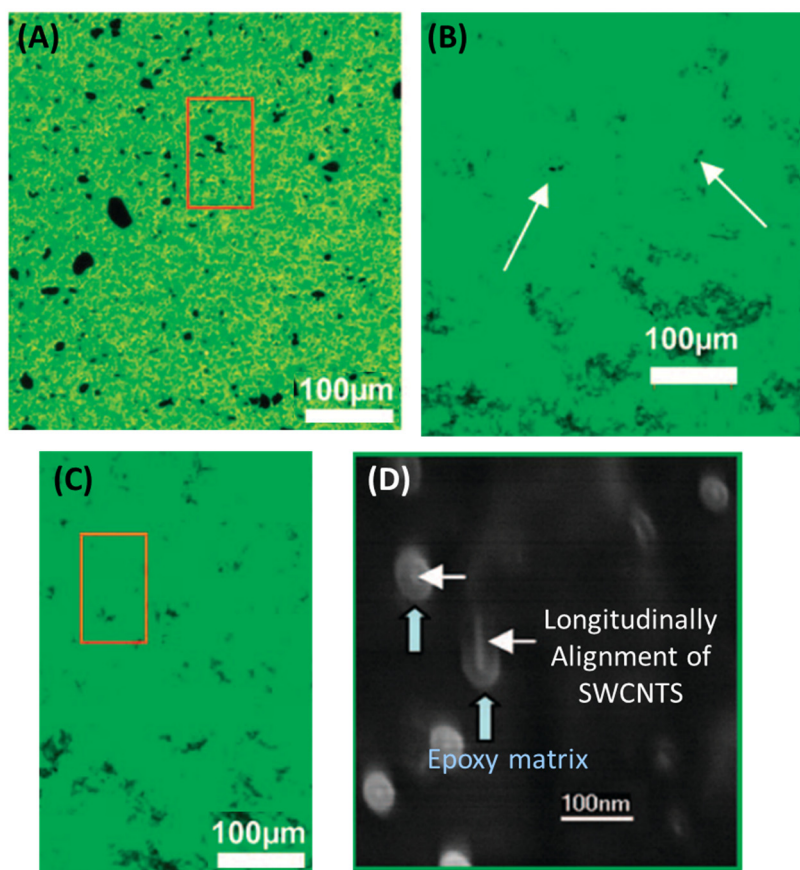


Figure 5. Microscopic images of (A) poly(amidoamine)-free single-walled carbon nanotube-based epoxy matrix, PAMAM/SWCNTs/EP, with (B) 1 and (C) 2 as number generation and (D) field emission scanning electron microscope (FESEM) images of PAMAM/SWCNTs/EP with grafting generation 2 (Reprinted (adapted) with permission from Che, J.; Yuan, W.; Jiang, G.; Dai, J.; Lim, S.Y.; Chan-Park, M.B. Epoxy Composite Fibers Reinforced with Aligned Single-Walled Carbon Nanotubes Functionalized with Generation 0–2 Dendritic Poly(Amidoamine). *Chem. Mater.* **2009**, *21*, 1471–1479 [22]. Copyright (2020) American Chemical Society.).

The fabrication of nanocomposites involving vertically aligned (VA) CNTs as fillers has also been studied and has strong potential for future biochemical sensors and water treat membranes. Macdonald et al. [16] reported an ultrasonically assisted “grafting-from” RAFT polymerization of the monomer styrene in the presence of VA-SWCNTs on a silicon substrate. This involved two main steps: the VA-carboxylated SWCNTs, obtained via sulfuric and nitric acid treatment, were bonded to the substrate surface by the formation of an ester linkage between the carboxyl and hydroxyl groups from the VA-SWCNTs and substrate, respectively. Then, the sidewalls of SWCNTs were covalently functionalized with bis(dithioester) groups acting as CTAs to initiate the “grafting-from” polymerization of the styrene. The vertical preservation of VA-SWCNTs within the polystyrene matrix on the substrate was confirmed by atomic microscopy force microscopy (AFM) analysis, as depicted in Figure 6. Ul Haq et al. [23] performed the grafting-from polymerization of the monomer aniline in the presence of nitrogen-doped VA-CNTs and showed the conservation of the vertical alignment of carbon nanotubes during the polymerization, as depicted in Figure 7. They showed that the nitrogen-doped sites present in the CNTs walls acted as nucleation sites for the initiation of the aniline polymerization. The incorporation of metal oxides such as manganese or ruthenium oxide in the previous nanocomposites allows them to be used as supercapacitor electrodes because of their synergetic proprieties.

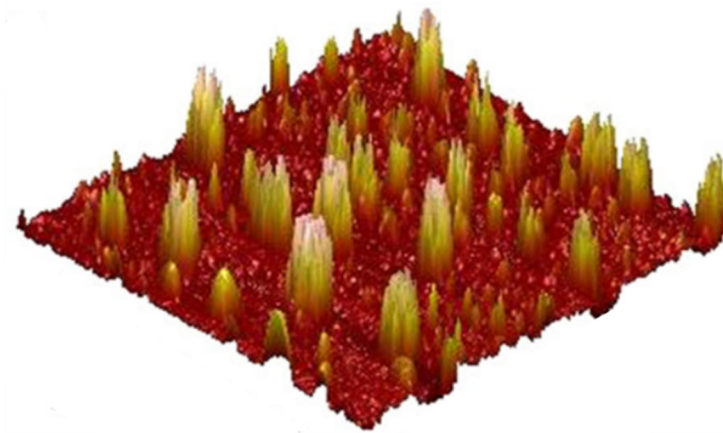


Figure 6. Atomic force microscopy (AFM) image of vertically aligned (VA)-SWCNTs/polystyrene (PS) nanocomposites (Reprinted from Macdonald, T.J.; Gibson, C.T.; Constantopoulos, K.; Shapter, J.G.; Ellis, A.V. Functionalization of Vertically Aligned Carbon Nanotubes with Polystyrene via Surface Initiated Reversible Addition Fragmentation Chain Transfer Polymerization. *Appl. Surf. Sci.* **2012**, *258*, 2836–2843 [16], with permission (2020) from Elsevier).

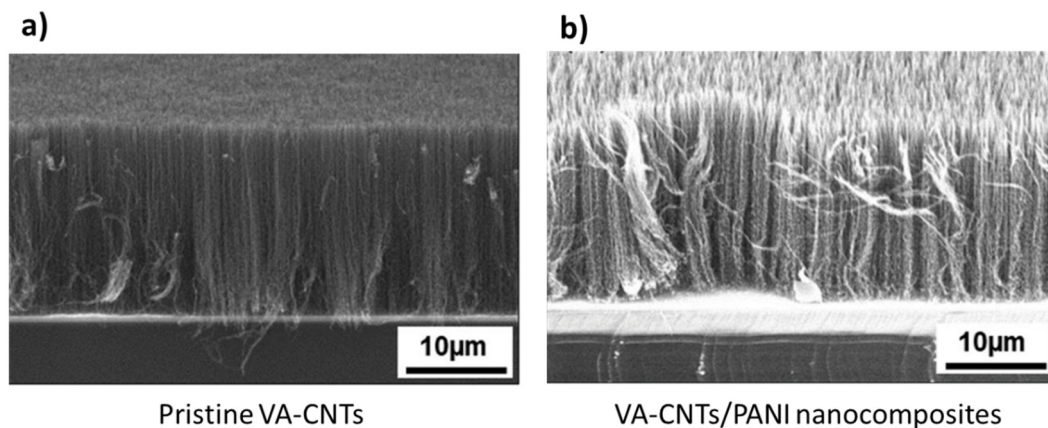


Figure 7. FESEM images of VA-CNTs (a) before and (b) after the grafting of polyaniline by a grafting-from method (Reprinted from Haq, A.U.; Lim, J.; Yun, J.M.; Lee, W.J.; Han, T.H.; Kim, S.O. Direct Growth of Polyaniline Chains from N-Doped Sites of Carbon Nanotubes. *Small* **2013**, *9*, 3829–3833 [23], with permission (2020) from WILEY).

Besides enabling greater efficiency in achieving very homogenous CNT dispersion, ultrasonication also makes it possible to create highly reactive species in a medium, thus obviating the need for chemical initiators during the polymerization. Koshio et al. [24] drew attention to defects on the SWCNT sidewalls in a monochlorobenzene (MCB) solution of poly(methyl methacrylate) (PMMA) during ultrasonication. In addition to the fact that these defects acted as reactive sites, other reactive groups were produced through the solvent and polymer decomposition, resulting in a covalent attachment of PMMA to the CNT surface. Applying ultrasound waves in an aqueous medium generates highly reactive radicals which may then initiate the polymerization reaction [11]. Mutharania et al. [25] described an initiator-free polymerization of the monomer N-isopropyl acrylamide (NIPAM) in the presence of the crosslinker *N,N'*-methylene-bis-acrylamide (MBA) under the application of an ultrasonication power of 400 W into deionized water. The transient collapse of bubbles produced hydroxyl radicals which acted as initiators. Thus, the “grafting-from” polymerization of NIPAM onto the carbon nanofiber (CNF) surface was initiated by both the covalent introduction of chemical initiator moieties (azobisisobutyronitrile, AIBN) onto the CNFs, and the creation of hydroxyl radicals under ultrasonication that promoted the polymerization. The characteristic temperature-sensitivity of the

resulting polymer combined with the CNFs' conductive properties due to the presence of defects make these nanocomposites very promising as electrochemical sensors.

2.1.2. Grafting-From through Inverse Emulsion Polymerization

Multiple studies have described the introduction of CNT into a polyaniline (PANI) matrix, since PANI is one of the most common electrically conductive polymers. When combined with carbon nanotubes (CNT), the resulting composites lead to considerable enhancement in terms of their mechanical, electric and optoelectrical properties [3]. PANI is a frequent choice because of its ease of synthesis, versatile properties, and its low-cost monomer [26]. In situ inverse emulsion polymerization is one of the most widely employed modes of fabrication of these nanocomposites.

Suckeveriene et al. [27] developed nanocomposites based on PANI in the presence of MWCNTs. The surfactant Camphor-10-sulfonic acid (β) (CSA) was dissolved in chloroform to which a distilled aniline solution and ammonium persulfate (APS) were added, followed by MWCNTs, either in situ (before polymerization) or ex situ (after polymerization) and then were sonicated. The morphology evidenced by Cryo-TEM showed that the MWCNT nanotubes were well-coated by PANI, resulting in a core-shell structure for both PANI/ MWCNT in situ and ex situ with an average diameter of ~50 nm for the in situ. The dispersions displayed long term stability (several months) and low resistivity, thus confirming the formation of MWCNT-PANI interactions.

Zelikman et al. [28] developed a new, rapid in situ dynamic inverse emulsion polymerization process under sonication resulting in stable nanocomposite PANI/MWCNTs in which MWCNTs were coated by PANI, leading to uniform PANI/ MWCNT tubes with an average diameter of ~37 nm, as shown in high resolution scanning electron microscope (HRSEM) images (Figure 8). The aqueous phase containing the APS radical initiator was added in the continuous phase containing aniline (monomer), dodecyl benzene sulfonic acid (DBSA, dopant), MWCNTs and toluene (solvent). The presence of MWCNTs enhanced the mechanical properties and electrical conductivity.

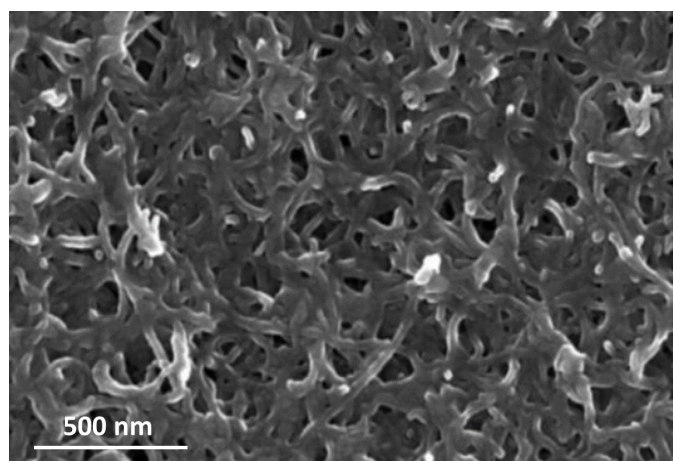


Figure 8. High resolution scanning electron microscopy (HRSEM) image of MWCNT/PANI nanocomposites prepared by ultrasonically induced inverse emulsion polymerization (Reprinted from Zelikman, E.; Suckeveriene, R.Y.; Mechrez, G.; Narkis, M. Fabrication of Composite Polyaniline/CNT Nanofibers Using an Ultrasonically Assisted Dynamic Inverse Emulsion Polymerization Technique. *Polym. Adv. Technol.* **2009**, *21*, 150–152 [28], with permission (2020) from WILEY).

They also tested other types of single-walled and double-walled carbon nanotubes, all of which were coated with PANI at a thickness of 11–34 nm [18]. a two-point probe technique showed that the PANI/CNT composites exhibited high film resistivity and light transparency and a decrease in haze as the film's thickness decreased [18].

Brook et al. [29] also carried out in situ inverse emulsion polymerization followed by either precipitation-filtration or a drop-cast step to produce nanocomposite PANI/CNT within a styrene-isoprene-styrene (SIS) block copolymer elastomeric matrix, as depicted in Figure 9. They showed that the precipitation-filtration method was significantly more efficient for the generation of a continuous well-organized three-dimensional CNT network [29].

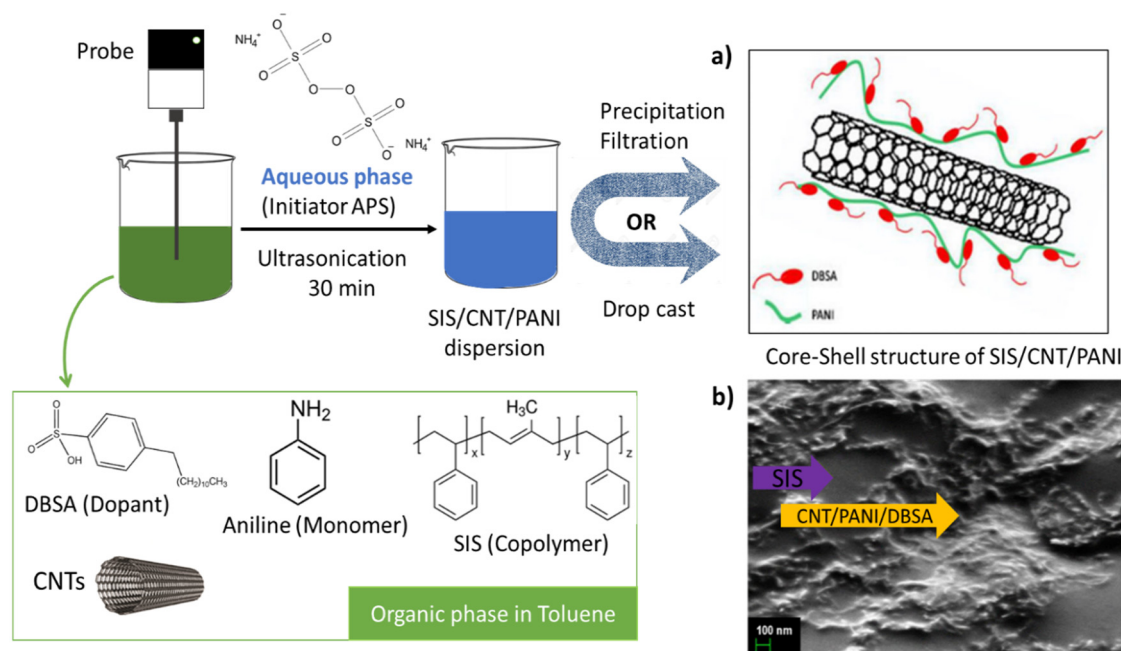


Figure 9. Fabrication via in situ inverse emulsion polymerization of the styrene=isoprene-styrene (SIS)/CNT/PANI elastomeric nanocomposite film by precipitation-filtration or drop-casting and (a) schematic structure of the resulting composites and (b) HRSEM images (Reprinted from Brook, I.; Mechrez, G.; Suckeveriene, R.Y.; Tchoudakov, R.; Lupo, S.; Narkis, M. The Structure and Electro-Mechanical Properties of Novel Hybrid CNT/PANI Nanocomposites. *Polym. Compos.* **2014**, *35*, 788–794 [29]; and from Brook, I.; Mechrez, G.; Suckeveriene, R.Y.; Tchoudakov, R.; Lupo, S.; Narkis, M. Electrically Conductive Hybrid Elastomeric Nanocomposites. *Composites* **2013**, *161*, 1–3 [30], with permission (2020) from WILEY).

Brook et al. [30] also produced a core-shell nanostructure in which CNT was wrapped by PANI as seen in the HRSEM images and the fact that elastomeric ‘islands’ of SIS block copolymer were created (Figure 9). The use of PANI enabled the CNT to be well separated from each other, thus forming a stable dispersion when prevented from agglomerating (fewer Van der Waals interactions). The percolation threshold was low (~ 0.4 by weight) due to the formation of these islands. They also showed that adding CNT considerably enhanced the mechanical properties which could later be tuned as a function of the CNT filler [30]. a very high Young’s modulus was reported, along with a decrease in strain at break for CNT loadings between 3 and 7 wt%, whereas lower mechanical properties were obtained for higher loadings. Tailoring the CNT content also had an impact on the composite’s morphology; according to the HRSEM images, the nanocomposites with low CNT content exhibited a more open network with larger-sized elastomeric islands.

A four-point probe technique showed that the composite displayed high conductivity ($\sim 4 \text{ S cm}^{-1}$) by forming continuous three-dimensional CNT/PANI networks [31]. They also tested the effectiveness of a three-dimensional segregated conductive SIS/CNT/PANI nanocomposite network as an electro-mechanical strain sensor for two different elastomers: SIS-14% and SIS-22% [32]. The mechanical properties (Young’s modulus and stress at break) were much higher with SIS-22% than with SIS-14%. Both sensors displayed a uniform homogeneous relative resistance amplitude, but there

was better relative resistance with the tougher matrix. However, the sensor containing the softer SIS exhibited greater sensitivity because of the weaker π – π interactions between the CNT and the polymer matrix. The sensors were also more sensitive closer to the percolation threshold.

Suckeveriene et al. [33] reported the synthesis of a nanotube/poly(styrene-co-acrylamide) composite fabricated by dynamic interfacial emulsion polymerization without using a surfactant, under sonication in which the acrylamide fraction attached to the CNT hydrophilic surfaces. The result was a stable, uniform dispersion, and a clear transparent coating prepared from the previous dispersion.

2.2. Graphene-Based Nanocomposites

Ultrasonically induced polymerization of the monomer aniline in the presence of graphene nanoparticles has also been widely studied. Various approaches have been explored to fabricate these nanocomposites. Regueira et al. [34] produced PANI/graphene nanocomposites by implementing an in situ inverse emulsion polymerization under sonication of aniline in the presence of graphene sheets in chloroform. The initiator APS containing the aqueous phase was added to the organic phase comprising the dopant DBSA, the distilled aniline, and the graphene sheets in a chloroform medium. The graphene sheets were well dispersed in the PANI resulting in a wrapping of graphene by the PANI matrix as shown by the Cryo-TEM images. The TGA images indicated that the composite had higher thermal stability as the graphene content increased. This also pointed to the nanocomposite's potential to be used as an electro-mechanical sensor since the electrical resistivity decreased under pressure as a result of its high graphene content, thus leading to an increase in electric conduction.

PANI can also be grafted onto the surface of graphene by first covalently functionalizing the graphene sheets from which the in situ polymerization is initiated. Nguyen et al. [35] functionalized reduced graphene oxide (rGO), prepared by a modified Hummers method with amine groups under acidic conditions. These reactive moieties located on the surface graphene were used to initiate the growth of aniline chains, resulting in a uniform grafting of PANI on the graphene surface as proved by SEM and TEM. Modification of monomer molecules can also be a way to functionalize graphene for the fabrication of nanocomposites. Park et al. [13] modified the monomer aniline with perfluorophenyl azide (PFPA) molecules through a coupling reaction confirmed by Fourier-transform infrared spectroscopy (FTIR). Then, the resulting modified-aniline chains were covalently attached to the surface of few-layer graphene (FLG) flakes by microwave-heating. Subsequently, the in situ grafting polymerization of aniline was produced out of modified-aniline functionalized FLG flakes, mediated by APS under sonication, leading to a homogenous vertical grafting of PANI (needle-like structures) on the FLG flakes; the grafted PANI amounted to ~26%. an enhancement of the capacitance within the PANI/graphene nanocomposites was demonstrated by cyclic voltammetry that confirmed the preservation of electrochemical properties after grafting.

The natural tendency of graphene sheets to entangle because of π – π stacking interactions between different layers is a real issue for the production of stable graphene-based nanocomposites exhibiting high chemical-physical performance. The covalent attachment of the polymer onto the graphene surface appears to be an efficient method to achieve good dispersion of graphene within the matrix. Xu et al. [36] successfully demonstrated good dispersion of GO within a hyperbranched polymer (HP) matrix by an in situ “grafting-from” ROP. Prior to the in situ polymerization of the cyclic ether monomer 3-ethyl-3-oxetanethanol initiated by boron trifluoride etherate in the presence of GO, a stable GO dispersion in chloroform was achieved by ultrasonication, resulting in well separated graphene sheets. The HPs grafted to GO were found to have better thermal stability than pristine HPs as well as enhanced mechanical properties including higher tensile strength. an excellent surface contact between the carbon fillers and the polymer also made it possible to obtain very good filler dispersion within the matrix. Xu et al. [17] showed that the high content of polymer nylon-6 (PA6) chains (~78%) grafted onto the rGO surface resulted in improved interfacial contact because of the strong interactions between the carboxylic groups from rGO and the amino moieties located at the PA6 chain ends. This high grafting was achieved through an ultrasonically assisted in situ ROP of the monomer caprolactam

initiated by 6-aminocaproic acid in the presence of GO, which was thermally reduced during the polycondensation, resulting in brush-like PA6 chains that were highly grafted onto the rGO sheets. By using the in situ polymerization approach, the monomer molecules were located between the different exfoliated graphene sheets, thus preventing the re-stacking of the graphene layers during polymerization. The formation of fibers from the resulting composites by melt spinning demonstrated enhanced thermal and mechanical properties including a high Young's modulus and tensile strength.

3. Non-Covalent Interactions

The non-covalent attachment of carbon nanoparticles to a polymeric matrix (adsorption) is mainly based on Van der Waals, π - π stacking and hydrogen bond forces [37]. Numerous methods have been developed to prepare CNTs or graphene-based nanocomposites by the non-covalent approach to overcome the main drawback of covalent functionalization: the loss of the intrinsic properties of CNTs and graphene as a result of perturbation of the sp^2 structure [12]. Besides the efficiency of the chemical functionalization that involves the use of strong acid, one major issue is the emergence of defects on the nanocarbon surface which inevitably alters its structural properties. Park et al. [38] proved that non-covalent CNTs functionalized by hydrophobic pyrene molecules preserved the inherent properties of CNTs, whereas when using acidic-treated-CNTs (covalent functionalization), a greater number of defects appeared, thus lowering the electrical properties of the poly(3-hexylthiophene)-based nanocomposites in the presence of the CNTs.

3.1. CNT-Based Nanocomposites

CNTs possess extraordinary properties including a high aspect ratio and electrical conductivity, which make them excellent candidates for a variety of applications such as sensors, storage, for example. However, the resulting nanocomposites can suffer from the natural tendency of nanotubes to agglomerate due to strong Van der Waals forces, which results in the poor dispersion of CNTs into the polymeric matrix. In situ polymerization associated with ultrasonication is one way to overcome this drawback. SWCNTs have been successfully dispersed into an aromatic polyimide matrix through the in situ polymerization of the monomers 1,3-bis(3-aminophenoxy) benzene (APB) and 2,2-bis(3,4-anhydrodicarboxyphenyl) hexafluoro- propane (6 FDA) under ultrasonication [39]. The authors reasoned that the cavitation phenomenon overcame the agglomeration of SWCNTs, and that the decrease in Brownian motion was due to the high viscosity of the solution. The choice of initiator for polymerization also controls CNT dispersion. Li et al. [40] selected a porphyrin-based zinc complex initiator to carry out the ring-opening polymerization of lactide in the presence of CNTs in tetrahydrofuran, while also serving as mediator to bind CNTs to the resulting polylactic acid polymer. They reported that strong π - π stacking interactions were formed between the porphyrin molecules and CNTs, resulting in CNTs embodied in the matrix through non-covalent binding (observed using FTIR, UV-Vis, and fluorescence spectroscopy).

Although in situ polymerization is widely used to create carbon-based nanocomposites based on the adsorption of carbon fillers in the matrix, other techniques such as melt-mixing can be considered. Hsiao et al. [41] reported the uniform wrapping of multi-walled carbon nanotubes (MWCNTs) within a polyethylene-based matrix. First, MWCNTs were functionalized by a copolymer dispersant synthesized from the monomers of phenyl methacrylate and glycidyl methacrylate, followed by grafting with amine. The optimal weight ratio of the MWCNTs to the polymer dispersant was found to be 1:0.75. Then, they cured the wrapped CNTs and the resulting powder was extruded with polyethylene (PE). They demonstrated the efficiency of the polymer dispersant in preventing the agglomeration of CNTs by reducing the Van der Waals interactions. The CNT/PE nanocomposites showed low surface resistivity, leading to high conductivity, making them good potential electromagnetic and electrostatic shields.

3.2. Graphene-Based Nanocomposites

The preparation of conjugated polymer-based nanocomposites in the presence of carbon can be achieved by in situ polymerization. This technique enables conductive polymers (CPs) to overcome their poor processability and solubility [42] by mixing the carbon materials with the monomers and then polymerizing them. Sahoo et al. [6] reported the fabrication of nanocomposites by in situ polymerization of two different CPs, polypyrrole (PPy) and polyaniline (PANI), in the presence of graphene. They investigated the role of graphene as a nano-reinforcement filler and reported significant improvement in thermal properties with FTIR, XPS and TGA, as well as in its electrical properties as shown by a four-point probe. The graphene surface was first functionalized by amine groups covalently linked to the graphene's carbon atoms using an ethylenediamine (EDA) and dicyclohexylcarbodiimide (DCC)-based solution in THF, following its acidic treatment, which resulted in modified graphene. The grafting of the amine groups on the graphene surface was demonstrated by the presence of peaks characteristic of N-H and C-N group vibrations by FTIR, which was confirmed by XPS analysis. The nanocomposites were synthesized by in situ polymerization in three steps. First, a suspension of modified-graphene and cetyltrimethylammonium bromide (CTAB), acting as surfactant was sonicated with distilled water. In the second step, aniline or pyrrole monomers were added to the previous solution. To initiate the polymerization, ammonium persulphate (APS), which also acted as an oxidant, was sonicated with the solution from the second step. Polymerization took 24 h at 0–5 °C, resulting in PANI-based modified graphene (MGA) or PPy-based modified graphene (MGP) nanocomposites. a schematic diagram (Figure 10) illustrates these three steps. The use of sonication (first step) allowed the graphene sheets to be broken down, which promoted the electrostatic interactions with the monomers (second step). Then, the addition of APS initiated the polymerization from monomer molecules absorbed on the graphene sheets.

The field emission scanning electron microscope (FESEM) images (Figure 11) show that regardless of the type of monomer used, the polymer covering of the graphene sheets was much more uniform for the modified graphene-based nanocomposites than for pure graphene-based nanocomposites. This may be attributed to the establishment of hydrogen bonding or π – π stacking between amino groups from the modified-graphene and the monomer molecules. Furthermore, in the case of unmodified graphene, polymerization also occurred outside the graphene, as schematically depicted in Figure 10B.

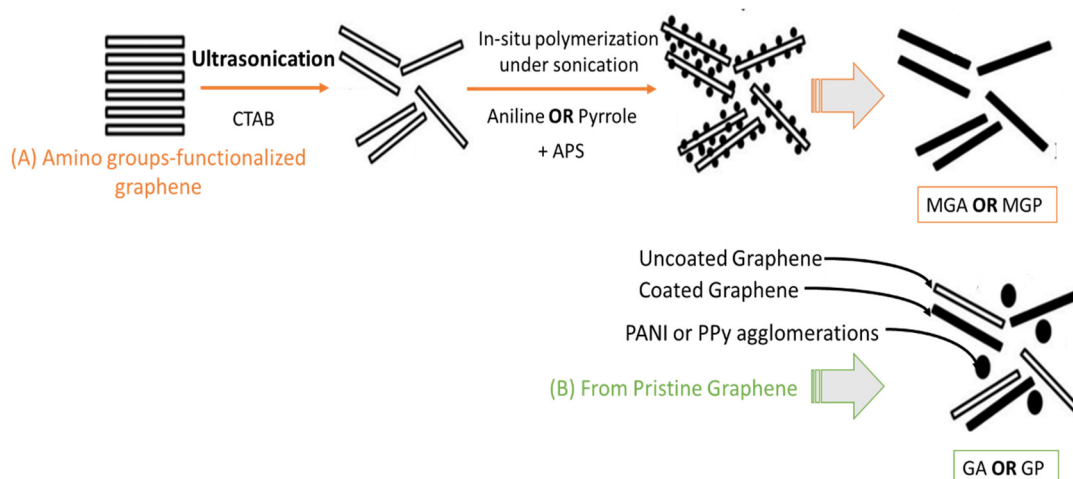


Figure 10. Preparation of PANI-based modified graphene (MGA) or PPy-based modified graphene (MGP) nanocomposites using (A) modified graphene and (B) pristine graphene yielding PANI/Graphene (GA) and PPy/Graphene (GP) (Reprinted from Sahoo, S.; Bhattacharya, P.; Hatui, G.; Ghosh, D.; Das, C.K. Sonochemical Synthesis and Characterization of Amine-Modified Graphene/Conducting Polymer Nanocomposites. *J. Appl. Polym. Sci.* **2012**, *128*, 1476–1483 [6], with permission (2020) from WILEY).

It is clear that the thermal properties of nanocomposites were enhanced by the incorporation of modified graphene (the weight loss at 200 °C due to PPy decomposition was a little higher than in the pristine graphene-based materials, according to the TGA curves [6]). In addition, an improvement in electrical conductivity in the presence of modified graphene was shown by a four-point probe measurement system. Specifically, the MGA nanocomposites had a higher conductivity value (8.12 S/cm). The increase in conductivity may be linked to the π – π stacking between the graphene sheets and polymers as well as the uniform coating of the polymers.

There are several ways to produce carbon-based composites films, but the preferred methods are the layer-by-layer (LBL) assembly technique and in situ polymerization. The LBL assembly involves the superposition of different oppositely charged layers on a substrate, resulting in multilayered films [43]. This technique involves electrostatic interactions between the nanocarbon fillers and polymers. The fabrication of poly(vinyl alcohol) (PVA) film based on alternating deposits of the negatively charged graphene oxide (GO) and the positively charged polymer, polyethyleneimine (PEI), was reported in [44]. The functionalization of GO involved introducing negatively charged oxygen-containing groups onto its surface through the non-covalent attachment of phenoxycyclophosphazene (HPTCP), a phosphorus-nitrogen compound. an important step prior to the polarity change of GO is exfoliation followed by sonication. The combination of these two steps allowed the graphene sheets to be well-separated from each other, thus preserving their properties. The self-assembly of these different layers was governed by π – π stacking interactions. In addition, one of main advantages of employing non-covalent functionalization is the very good conservation of the layered structure of graphene within the coated PVA film, which endows the PVA membrane with high flexibility. Although the LBL technique makes it possible to control the thickness of composite films and achieve uniform multilayers, this process demands a considerable amount of materials and is a lengthy process [37].

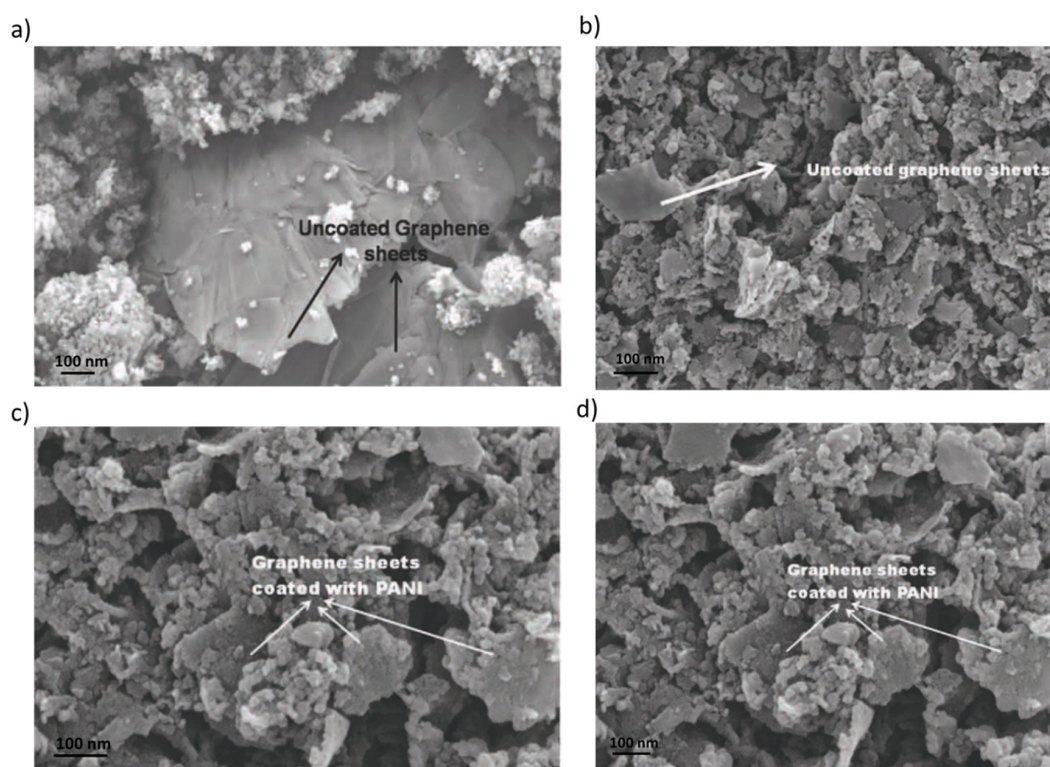


Figure 11. FESEM images of pristine graphene-based nanocomposites wrapped with (a) PANI and (b) PPy and modified graphene-based with (c) PANI and (d) PPy, at a magnification of 260.00 KX except for (a) 200.00 KX (Reprinted from Sahoo, S.; Bhattacharya, P.; Hatui, G.; Ghosh, D.; Das, C.K. Sonochemical Synthesis and Characterization of Amine-Modified Graphene/Conducting Polymer Nanocomposites. *J. Appl. Polym. Sci.* **2012**, *128*, 1476–1483 [6], with permission (2020) from WILEY).

An alternative to the production of nanocomposite films based on non-covalent interactions is the use of in situ polymerization. a polyamide-based film in the presence of a graphene/polyaniline (PANI) composite prepared by a non-covalent approach was reported in [45]. The first step was the ultrasonically assisted polymerization of the monomer aniline in the presence of exfoliated graphene under acidic conditions. Then, the in situ polymerization took place in a mixture containing the previous mixture and the monomers 4,40-diaminodiphenyl ether (ODA) and pyromellitic dianhydride (PMDA). Finally, the resulting dispersion was cast on a glass substrate to form the graphene-polyaniline/polyimide composite film. The dispersion graphene-PANI was found to be stable as a result of the π - π interactions between the two components. As displayed by the SEM images (not shown), PANI uniformly coated the graphene surface, preventing the agglomeration of graphene sheets and resulting in a polyamide film with high electrical properties which could serve as electromagnetic interference shield.

Tian et al. [46] described the non-covalent decoration of graphene oxide using hyperbranched polyesters (HBP) to form GO-based epoxy resin nanocomposites. a GO dispersion was ultrasonicated into an HBP medium at 24 °C for one hour, and then filtered and washed, resulting in hyperbranched polyester functionalized GO (HBP-GO). Subsequently, this mixture was mixed with epoxy resin, and then cast. FTIR analysis demonstrated the adsorption of HBP into GO sheets, with a load of about ~38% (TGA results). The non-restacking of graphene sheets was prevented by the steric hindrance between the carboxyl groups from the polyesters. Besides the good dispersion due to the π - π stacking forces, the nanocomposites showed good interfacial contact and an enhancement of mechanical properties, i.e., high microhardness, and elastic modulus.

4. Binary Filler-Based Nanocomposites

Several research groups have investigated the effects of using a combination of two different carbon nanomaterials (binary fillers) on the properties of the resulting nanocomposites. Patole et al. [7] investigated the thermal and mechanical properties of graphene-based composites by incorporating carbon nanotubes. They developed a new method combining the incorporation of binary fillers (i.e., a combination of graphene particles and carbon nanotubes) into a polymer matrix through in situ microemulsion polymerization.

They synthesized graphene/CNT/polystyrene nanocomposites as follows. an aqueous suspension of graphene and multi-wall carbon nanotubes (MWCNTs) was prepared by sonication, and then added to a reactor containing a mixture of monomer styrene, crosslinking divinylbenzene (DVB) and the initiator AIBN. Polymerization took 4 h at 85 °C. Afterwards, the PS (polystyrene) films were prepared from the graphene/CNT/polystyrene nanocomposites as shown in Figure 12. This resulted in an interconnected network in which the PS-grafted MWCNTs acted as a bridge to bind the graphene sheets to each other and connect the MWCNTs and the graphene via PS chains (SEM and TEM images in Figure 13), which considerably enhanced its thermal and mechanical, but especially its elastic properties (high modulus). This procedure also led to a decrease in the sheet resistance, i.e., an increase in the electrical conduction within the composite film.

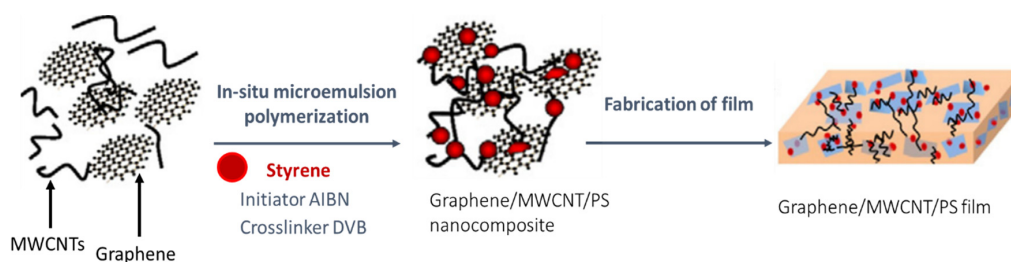


Figure 12. Preparation flow for graphene/MWCNT/PS film using divinylbenzene (DVB) crosslinker (Reprinted from Patole, A.S.; Patole, S.P.; Jung, S.-Y.; Yoo, J.-B.; An, J.-H.; Kim, T.-H. Self Assembled Graphene/Carbon Nanotube/Polystyrene Hybrid Nanocomposite by in Situ Microemulsion Polymerization. *Eur. Polym. J.* **2012**, *48*, 252–259 [7], with permission (2020) from Elsevier).

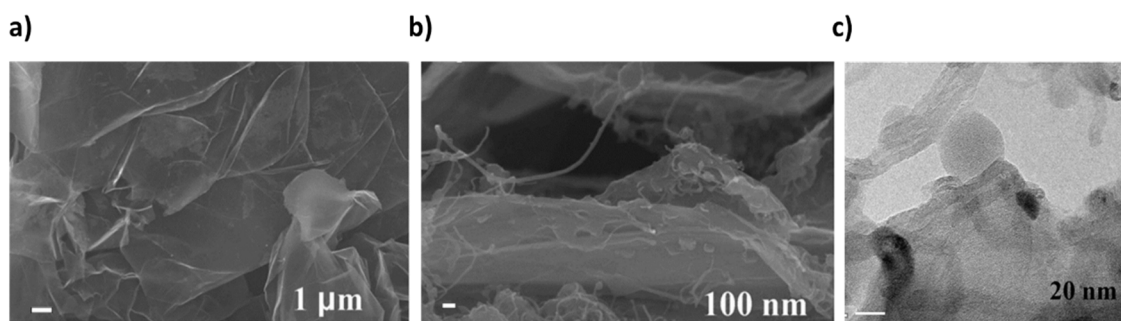


Figure 13. (a) SEM image of exfoliated graphene and the graphene/MWCNT/PS nanocomposites prepared by in situ micro-emulsion polymerization observed by (b) SEM and (c) TEM (Reprinted from Patole, A.S.; Patole, S.P.; Jung, S.-Y.; Yoo, J.-B.; An, J.-H.; Kim, T.-H. Self Assembled Graphene/Carbon Nanotube/Polystyrene Hybrid Nanocomposite by in Situ Microemulsion Polymerization. *Eur. Polym. J.* **2012**, *48*, 252–259 [7], with permission (2020) from Elsevier).

Patole et al., used gel permeation chromatography (GPC) to evaluate the effect of binary fillers on two important polymerization parameters: molecular weight (MW) and the polydispersity index (PDI) of polystyrene. The results showed that the use of graphene and MWCNTs increased the molecular weight (~40,000 and ~65,000 g/mol for neat PS and nanocomposites, respectively) so that the binary fillers contributed to consuming the initiator. In this case, the quantity of the initiator diminished in the medium, which thus slowed down the formation of new polymer chains on the surface of the MWCNTs. Similarly, the PDI of the PS chains increased in the nanocomposites (~168,000 and ~228,000 for the neat PS and nanocomposites, respectively), because most of the PS nanoparticles were grafted to the MWCNTs and not to the graphene layers. Brownian motion is likely to have removed the absorbed surfactant SDS on the surface of the fillers, thus creating new active radical centers enabling the initiation of the polymerization reaction.

Zhang et al. [47] fabricated anti-corrosion coating based on an urushiol formaldehyde polymer (UFP) in the presence of graphene oxide and multiwalled carbon nanotubes (GO/MWCNTs/UFP), which could be used in a marine environment. The two main steps consisted of in situ polymerization of UFP in the presence of MWCNTs followed by the incorporation of modified graphene oxide (MGO) in blending the MWCNTs/UFP.

A mixture of urushiol and formaldehyde was prepared in xylene at 90 °C. Once the temperature dropped to 60 °C, an ultrasonicated treated solution of MWCNTs was added, producing MWCNTs/UFP (UFP to MWCNTs 100:1). The polymerization temperature ranged from 90 to 130 °C. FTIR analysis indicated that the in situ polymerization worked efficiently as a result of the decrease in the intensity of the characteristic peaks of O-H groups, proving the existence of chemical bonding between the OH groups from MWCNTs and the phenyl ring of the UFP. Then, an ultrasonicated-treated suspension of MGO, functionalized by silanization from graphene oxide with 3-aminopropyltriethoxysilane (APTES) (Figure 14) was mixed with the MWCNTs/UFP solution using a solution-blending technique that produced the GO/MWCNTs/UFP composite. Through FTIR analysis, Zhang et al. concluded that the OH groups from MWCNTs reacted with the phenyl ring of the UFP and with both the carboxyl and hydroxyl groups of GO.

The SEM images (Figure 15) indicated that aggregates were formed in the MWCNTs/UFP composite as a result of strong interfacial interactions between the MWCNTs and the UFP. However, no aggregates were apparent in the GO/MWCNTs/UFP composite, thus evidencing the GO's effectiveness in preventing corrosion. After coating the silicon substrate with GO/MWCNTs/UFP, the SEM images revealed that the GO had agglomerated by establishing π - π interactions and Van der Waals forces between the GO and the polymer matrix, thus at the same time enhancing its adhesion. XPS analysis confirmed the results predicted by FTIR, i.e., the formation of covalent bonds between the OH groups of the MGO and the MWCNTs/UFP.

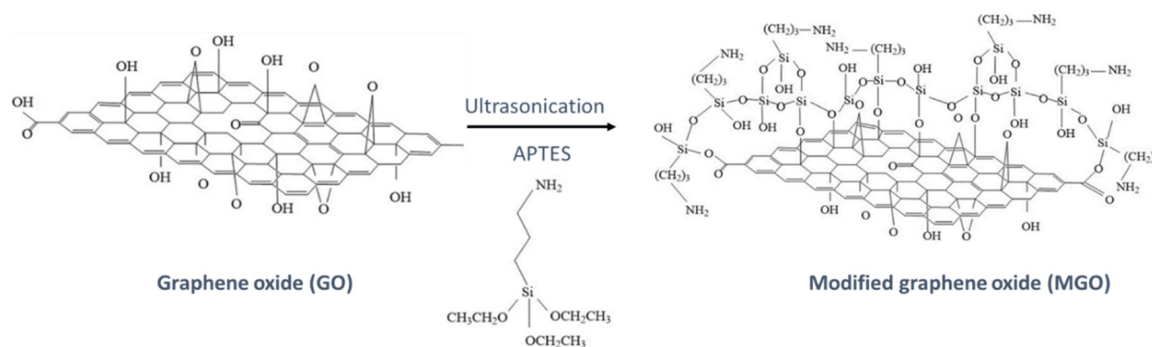


Figure 14. Fabrication of modified graphene oxide through ultrasonication assisted by silanization (Reprinted from Zhang, L.; Wu, H.; Zheng, Z.; He, H.; Wei, M.; Huang, X. Fabrication of Graphene Oxide/Multi-Walled Carbon Nanotube/Urushiol Formaldehyde Polymer Composite Coatings and Evaluation of Their PhysiCo-Mechanical Properties and Corrosion Resistance. *Prog. Org. Coatings* **2019**, 127, 131–139 [47], with permission (2020) from Elsevier).

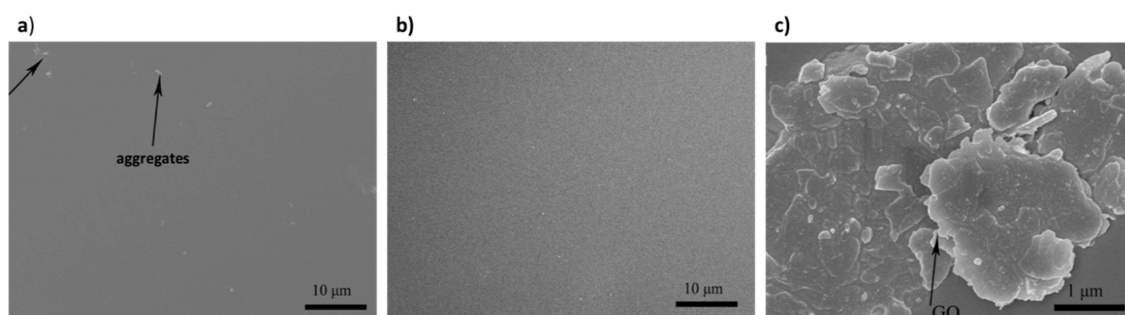


Figure 15. SEM images of (a) the MWCNTs/urushiol formaldehyde polymer (UFP) and (b) the GO/MWCNTs/UFP films (c) after its deposition on a silicon substrate (Reprinted from Zhang, L.; Wu, H.; Zheng, Z.; He, H.; Wei, M.; Huang, X. Fabrication of Graphene Oxide/Multi-Walled Carbon Nanotube/Urushiol Formaldehyde Polymer Composite Coatings and Evaluation of Their PhysiCo-Mechanical Properties and Corrosion Resistance. *Prog. Org. Coatings* **2019**, 127, 131–139 [47], with permission (2020) from Elsevier).

In terms of its physical-mechanical properties, several parameters have been studied including adhesion and hardness. The grade of hardness as well as adhesion were shown to be superior in the MGO/UFP composite as compared to the neat UFP, indicating that the graphene oxide allowed the MGO/UFP coating to enhance its scratch resistance. Although the incorporation of high concentrations of MWCNTs (1.0 wt.%) considerably decreased its hardness (H), the uniform dispersion of GO as nano-reinforcement into the MWCNTs/UFP matrix significantly enhanced hardness since it reached 6 H. The adhesion also improved, which Zhang et al. attributed to the creation of polar-polar interactions and H-bonding with polar groups from the metal substrate (Table 1). In addition, the corrosion protection efficiency (P.E.) of the GO/MWCNTs/UFP composite was found to be the highest (99.70%). The corrosion resistance of this composite coating was shown to be efficient; the surface was undamaged after immersion in a 10% NaOH solution for 14 days at room temperature. This indicates that graphene oxide is essential to MWCNTs/UFP coating because it enables the substrate to resist alkali conditions.

Palaznik et al. [48] have investigated the electrodynamic properties and the percolation threshold of composite materials based on polypropylene (PP) and a combination of carbon nanoparticles (graphene particles and carbon nanotubes). This composite polymer was synthesized by in situ polymerization mediated by the metallocene $\text{Me}_2\text{Si(2-Me-4-PhInd)}_2\text{ZrCl}_2$ activated by methylaluminoxane (MAO) which resulted in a high molecular weight PP.

Table 1. Physical-mechanical properties.

	Hardness	Adhesion	P.E. (%)
Neat UFP	3H	3	91.79
MGO/UFP	6H	2	99.45
MWCNTs/UFP	1H	1	99.69
GO/MWCNTs/UFP	6H	1	99.70

Hardness (maximum grade 6, minimum grade 1), adhesion (maximum grade 1, minimum grade 6) and corrosion protection efficiency (P.E.) of pure polymer UFP, MGO/UFP, MWCNTs/UFP and GO/MWCNTs/UFP films (Reprinted from Cheng, K.; Li, H.; Zhu, M.; Qiu, H.; Yang, J. In Situ Polymerization of Graphene-Polyaniline@polyimide Composite Films with High EMI Shielding and Electrical Properties. *RSC Adv.* **2020**, *10*, 2368–2377 [45], permission (2020) from the Royal Society of Chemistry).

They investigated two ways to produce binary fillers. In the first, two types of carbon nanotubes (either MWCNTs or SWCNTs) were mixed with thermally reduced graphite oxide (TRGO). In the second, an ultrasound-treated suspension of graphite oxide (GO) and SWCNT was freeze-dried and then heated to 900 °C. The two binary fillers were mixed and sonicated with MAO and toluene. The resulting suspensions were then added in propylene bulk, followed by the addition of the metallocene catalyst to mediate the polymerization (60 °C). The TEM images confirmed the presence of both graphene nanoplates (TRGO) and small island-shaped carbon nanotubes (MWCNT or SWCNT).

Palaznik et al., also used differential scanning calorimetry (DSC) to examine the thermophysical properties of composites as a function of content nanofillers. The incorporation of high content carbon nanoparticles led to a widening of the melting peak due to the nucleating step which probably prevented the development of larger crystalline areas and also led to a slight decrease in the enthalpy of melting, which corresponds to a decrease in crystallinity. The TGA data showed that the addition of carbon fillers improved the thermal stability of all the composite materials as well as the thermo-oxidative resistance. This was seen in the comparison of TRGO and nanocarbon particles (MWCNT or SWCNT) compared to the composite PP; specifically, for a TRGO+MWCNT filler content of 4.2 wt%, the oxidation rate was twice as low than for neat PP. Thus, the use of carbon nanotubes enables a better dispersion of graphene particles within the polymer matrix and leads to an increase in the oxidative resistance. An investigation of the mechanical properties of different composites showed that the introduction of anisotropic carbon nanofillers increased the elastic modulus (E) but markedly decreased the elongation of breaks. Palaznik et al., attributed this decrease to the formation of large pores and aggregates. The effects of content and type of filler on the relationship between conductivity and permittivity as well as the percolation threshold were also investigated. The percolation threshold decreased with the use of binary fillers (Table 2). The conductivity of TRGO/MWCNT or SWCNT-based composite materials was similar to monofiller-based materials at lower concentrations of TRGO nanoparticles. They concluded that SWCNT fillers conduct better than TRGO/MWCNT binary fillers whose conductivities were identical, and that the use of TRGO nanoparticles considerably increased permittivity, which was much higher for composite PP/TRGO/SWCNT than for PP/SWCNT.

Table 2. Comparison of mechanical properties.

	Elastic Modulus (E, MPa)	Break Elongation (ϵ_b , %)	Percolation Threshold (%)
Pure PP	1220	500	–
PP/TRGO	1555	7.8	3
PP/TRGO/MWCNTs	1710	5.7	2
PP/TRGO/SWCNTs	1390	11.2	–

Elastic modulus, break elongation and percolation threshold of pure polypropylene (PP), and graphene nanoplates (TRGO) nanocomposites (Reprinted from Tian, J.; Xu, T.; Tan, Y.; Zhang, Z.; Tang, B.; Sun, Z. Effects of Non-Covalent Functionalized Graphene Oxide with Hyperbranched Polyesters on Mechanical Properties and Mechanism of Epoxy Composites. *Materials* **2019**, *12*, 3103 [46], Open Access Materials MDPI.).

5. Conclusions

The incorporation of carbon nanotubes (SWCNT, MWCNT, graphene) into a polymer matrix considerably enhances the intrinsic properties of the polymer. These CNT-based nanocomposites exhibit excellent thermal, mechanical and physical properties which make them very promising for use in a wide range of fields from energy storage to optoelectronics to biomedical devices (electro-mechanical sensors, anti-corrosion coatings, etc.). Both non-covalent and covalent approaches can be employed. Although the non-covalent methods appear easier to perform, grafting in the presence of nanoparticles combined with ultrasonic polymerization can provide stronger CNT-polymer interactions and achieve a uniform and stable dispersion (breakdown of the nanoparticle agglomerates), the strong attachment of functional materials to the CNT surfaces, and a fine dispersion of CNT nanoparticles within the polymeric matrices. Nevertheless, the pathway to covalently functionalizing the nanocarbons requires the use of an acid mixture which affects the structural properties of the carbon materials within the nanocomposites, and hence their performance. The possibility of incorporating a high filler loading which could improve the interfacial interactions through covalent bonding between the carbon and the matrix would improve the physical properties of the nanocomposites. Inverse emulsion polymerization appears to be a possible alternative for the fabrication of covalent linkage-based nanocomposites because there is no need for prior acidic treatment of the CNTs. The non-covalent approach can also be considered when the aim is to avoid a structural perturbation of carbons, since achieving a good dispersion of carbon in the matrix is based on physical interactions (Van der Waals, π - π stacking and hydrogen bonds) that do not alter the intrinsic properties of carbon. However, this approach suffers from low structural stability.

Obtaining carbon-based nanocomposites with enhanced structural stability along with a decrease in sp^2 hybridized perturbation of carbon materials is a major challenge. The scale-up for fabrication of such composites can also be a hurdle, in particular for graphene-based nanocomposites because of the high cost of neat graphene. One solution would be to use reduced graphene oxide which is less oxygen-rich.

Hybrid nanocomposites possessing high properties can also be fabricated with other kinds of nanoparticles, and silica in particular due to its high surface area and its ability to form strong interactions with organic components such as the grafting of polystyrene chains onto a silica surface [4,49] or anti-fog molecules onto a methacrylic silica surface [50].

Funding: This research was partially supported by the Kinneret Academic College internal research fund.

Conflicts of Interest: The authors declare no conflict of interest.

References

1. Sattler, K.D. *Carbon Nanomaterials Sourcebook*; CRC Press: Boca Raton, FL, USA, 2016; Volume 1. [\[CrossRef\]](#)
2. Korotcenkov, G. *Handbook of Gas Sensor Materials: Properties, Advantages and Shortcomings for Applications*; Springer: New York, NY, USA, 2014. [\[CrossRef\]](#)
3. Suckeveriene, R.Y.; Zelikman, E.; Mechrez, G.; Narkis, M. Literature Review: Conducting Carbon Nanotube/Polyaniline Nanocomposites. *Rev. Chem. Eng.* **2011**, *27*, 15–21. [\[CrossRef\]](#)
4. Suckeverieme, R.Y.; Tzur, A.; Narkis, M.; Siegmann, A. Grafting of Polymer Chains onto Nano-Silica Particles via Peroxide Bulk Polymerization. *J Nanostructured Polym. Nanocomposites* **2007**, *3*, 13–21.
5. Ernould, B.; Devos, M.; Bourgeois, J.-P.; Rolland, J.; Vlad, A.; Gohy, J.-F. Grafting of a Redox Polymer onto Carbon Nanotubes for High Capacity Battery Materials. *J. Mater. Chem. A* **2015**, *3*, 8832–8839. [\[CrossRef\]](#)
6. Sahoo, S.; Bhattacharya, P.; Hatui, G.; Ghosh, D.; Das, C.K. Sonochemical Synthesis and Characterization of Amine-Modified Graphene/Conducting Polymer Nanocomposites. *J. Appl. Polym. Sci.* **2012**, *128*, 1476–1483. [\[CrossRef\]](#)
7. Patole, A.S.; Patole, S.P.; Jung, S.-Y.; Yoo, J.-B.; An, J.-H.; Kim, T.-H. Self Assembled Graphene/Carbon Nanotube/Polystyrene Hybrid Nanocomposite by in Situ Microemulsion Polymerization. *Eur. Polym. J.* **2012**, *48*, 252–259. [\[CrossRef\]](#)

8. Richards, W.T.; Loomis, A.L. The Chemical Effects of High Frequency Sound Waves I. a Preliminary Survey. *J. Am. Chem. Soc.* **1927**, *49*, 3086–3100. [\[CrossRef\]](#)
9. Thompson, L.H.; Doraiswamy, L.K. Sonochemistry: Science and Engineering. *Ind. Eng. Chem. Res.* **1999**, *38*, 1215–1249. [\[CrossRef\]](#)
10. Kaboorani, A.; Riedl, B.; Blanchet, P. Ultrasonication Technique: a Method for Dispersing Nanoclay in Wood Adhesives. *J. Nanomater* **2013**, *2013*, 1–9. [\[CrossRef\]](#)
11. Santos, H.M.; Lodeiro, C.; Capelo-Martínez, J.L. The Power of Ultrasound. *Ultrasound in Chemistry. Anal. Appl.* **2009**, 1–16, Chapter 1. [\[CrossRef\]](#)
12. Espinosa-González, C.G.; Rodríguez-Macías, F.J.; Cano-Márquez, A.G.; Kaur, J.; Shofner, M.L.; Vega-Cantu, Y.I. Polystyrene Composites with Very High Carbon Nanotubes Loadings by in Situ Grafting Polymerization. *J. Mater. Res.* **2013**, *28*, 1087–1096. [\[CrossRef\]](#)
13. Park, J.; Yang, X.; Wickramasinghe, D.; Sundhoro, M.; Orbey, N.; Chow, K.-F.; Yan, M. Functionalization of Pristine Graphene for the Synthesis of Covalent Graphene-Polyaniline Nanocomposite. *RSC Adv.* **2020**, *10*, 26486–26493. [\[CrossRef\]](#)
14. Saeb, M.R.; Najafi, F.; Bakhshandeh, E.; Khonakdar, H.A.; Mostafaiyan, M.; Simon, F.; Scheffler, C.; Mäder, E. Highly Curable Epoxy/MWCNTs Nanocomposites: an Effective Approach to Functionalization of Carbon Nanotubes. *Chem. Eng. J.* **2015**, *259*, 117–125. [\[CrossRef\]](#)
15. Bittmann, B.; Hauptert, F.; Schlarb, A.K. Ultrasonic Dispersion of Inorganic Nanoparticles in Epoxy Resin. *Ultrason. Sonochemistry* **2009**, *16*, 622–628. [\[CrossRef\]](#)
16. Macdonald, T.J.; Gibson, C.T.; Constantopoulos, K.; Shapter, J.G.; Ellis, A.V. Functionalization of Vertically Aligned Carbon Nanotubes with Polystyrene via Surface Initiated Reversible Addition Fragmentation Chain Transfer Polymerization. *Appl. Surf. Sci.* **2012**, *258*, 2836–2843. [\[CrossRef\]](#)
17. Xu, Z.; Gao, C. In Situ Polymerization Approach to Graphene-Reinforced Nylon-6 Composites. *Macromolecules* **2010**, *43*, 6716–6723. [\[CrossRef\]](#)
18. Suckeveriene, R.Y.; Mechrez, G.; Filiba, O.H.; Mosheev, S.; Narkis, M. Synthesis of Hybrid Polyaniline/Carbon Nanotubes Nanocomposites in Toluene by Dynamic Interfacial Inverse Emulsion Polymerization under Sonication. *J. Appl. Polym. Sci.* **2012**, *128*, 2129–2135. [\[CrossRef\]](#)
19. Marshall, N.; Sontag, S.K.; Locklin, J. Surface-Initiated Polymerization of Conjugated Polymers. *Chem. Commun.* **2011**, *47*, 5681–5689. [\[CrossRef\]](#) [\[PubMed\]](#)
20. Hou, W.; Zhao, N.-J.; Meng, D.; Tang, J.; Zeng, Y.; Wu, Y.; Weng, Y.; Cheng, C.; Xu, X.; Li, Y.; et al. Controlled Growth of Well-Defined Conjugated Polymers from the Surfaces of Multiwalled Carbon Nanotubes: Photoresponse Enhancement via Charge Separation. *ACS Nano* **2016**, *10*, 5189–5198. [\[CrossRef\]](#)
21. Yao, Z.; Braidy, N.; Botton, G.A.; Adronov, A. Polymerization from the Surface of Single-Walled Carbon Nanotubes—Preparation and Characterization of Nanocomposites. *J. Am. Chem. Soc.* **2003**, *125*, 16015–16024. [\[CrossRef\]](#)
22. Che, J.; Yuan, W.; Jiang, G.; Dai, J.; Lim, S.Y.; Chan-Park, M.B. Epoxy Composite Fibers Reinforced with Aligned Single-Walled Carbon Nanotubes Functionalized with Generation 0–2 Dendritic Poly(Amidoamine). *Chem. Mater.* **2009**, *21*, 1471–1479. [\[CrossRef\]](#)
23. Haq, A.U.; Lim, J.; Yun, J.M.; Lee, W.J.; Han, T.H.; Kim, S.O. Direct Growth of Polyaniline Chains from N-Doped Sites of Carbon Nanotubes. *Small* **2013**, *9*, 3829–3833. [\[CrossRef\]](#) [\[PubMed\]](#)
24. Koshio, A.; Yudasaka, M.; Zhang, M.; Iijima, S. a Simple Way to Chemically React Single-Wall Carbon Nanotubes with Organic Materials Using Ultrasonication. *Nano Lett.* **2001**, *1*, 361–363. [\[CrossRef\]](#)
25. Mutharani, B.; Ranganathan, P.; Chen, S.-M.; Kannan, R.S. Ultrasound-Promoted Covalent Functionalization of CNFs with Thermo-Sensitive PNIPAM via “Grafting-From” Strategy for On/Off Switchable Electrochemical Determination of Clothianidin. *Ultrason. Sonochemistry* **2019**, *56*, 200–212. [\[CrossRef\]](#) [\[PubMed\]](#)
26. Suckeveriene, R.Y.; Zelikman, E.; Narkis, M. *Hybrid Electrically Conducting Nanocomposites Comprising Carbon Nanotubes/Intrinsically Conducting Polymer Systems*; John Wiley & Sons, Inc.: Hoboken, NJ, USA, 2012.
27. Suckeveriene, R.Y.; Zelikman, E.; Mechrez, G.; Tzur, A.; Frisman, I.; Cohen, Y.; Narkis, M. Synthesis of Hybrid Polyaniline/Carbon Nanotube Nanocomposites by Dynamic Interfacial Inverse Emulsion Polymerization under Sonication. *J. Appl. Polym. Sci.* **2011**, *120*, 676–682. [\[CrossRef\]](#)
28. Zelikman, E.; Suckeveriene, R.Y.; Mechrez, G.; Narkis, M. Fabrication of Composite Polyaniline/CNT Nanofibers Using an Ultrasonically Assisted Dynamic Inverse Emulsion Polymerization Technique. *Polym. Adv. Technol.* **2009**, *21*, 150–152. [\[CrossRef\]](#)

29. Brook, I.; Mechrez, G.; Suckeveriene, R.Y.; Tchoudakov, R.; Lupo, S.; Narkis, M. The Structure and Electro-Mechanical Properties of Novel Hybrid CNT/PANI Nanocomposites. *Polym. Compos.* **2014**, *35*, 788–794. [[CrossRef](#)]
30. Brook, I.; Mechrez, G.; Suckeveriene, R.Y.; Tchoudakov, R.; Lupo, S.; Narkis, M. Electrically Conductive Hybrid Elastomeric Nanocomposites. *Composites* **2013**, *161*, 1–3.
31. Brook, I.; Mechrez, G.; Suckeveriene, R.Y.; Tchoudakov, R.; Narkis, M. a Novel Approach for Preparation of Conductive Hybrid Elastomeric Nano-Composites. *Polym. Adv. Technol.* **2013**, *24*, 758–763. [[CrossRef](#)]
32. Brook, I.; Tchoudakov, R.; Suckeveriene, R.Y.; Narkis, M. Electro-Mechanical Sensors Based on Conductive Hybrid Nanocomposites. *Polym. Adv. Technol.* **2015**, *26*, 889–897. [[CrossRef](#)]
33. Suckeveriene, R.Y.; Rahman, R.; Ovadia, M.; Szczupak, D.; Mechrez, G.; Narkis, M. Synthesis of Surfactant-Free Carbon Nanotube/Poly(Styrene-Co-acrylamide) by Dynamic Interfacial Emulsion Polymerization under Sonication. *Polym. Adv. Technol.* **2013**, *25*, 4–8. [[CrossRef](#)]
34. Regueira, R.; Suckeveriene, R.Y.; Brook, I.; Mechrez, G.; Tchoudakov, R.; Narkis, M. Investigation of the Electro-Mechanical Behavior of Hybrid Polyaniline/Graphene Nanocomposites Fabricated by Dynamic Interfacial Inverse Emulsion Polymerization. *Graphene* **2015**, *4*, 7–19. [[CrossRef](#)]
35. Van Hoa, N.; Lamiel, C.; Kharismadewi, D.; Tran, V.C.; Shim, J.-J. Covalently Bonded Reduced Graphene Oxide/Polyaniline Composite for Electrochemical Sensors and Capacitors. *J. Electroanal. Chem.* **2015**, *758*, 148–155. [[CrossRef](#)]
36. Xu, Q.; Gong, Y.; Fang, Y.; Jiang, G.; Wang, Y.; Sun, X.; Wang, R. Straightforward Synthesis of Hyperbranched Polymer/Graphene Nanocomposites from Graphite Oxide via in Situ Grafting from Approach. *Bull. Mater. Sci.* **2012**, *35*, 795–800. [[CrossRef](#)]
37. Ma, L.; Dong, X.; Chen, M.; Zhu, L.; Wang, C.; Yang, F.; Dong, Y. Fabrication and Water Treatment Application of Carbon Nanotubes (CNTs)-Based Composite Membranes: a Review. *Membranes* **2017**, *7*, 16. [[CrossRef](#)] [[PubMed](#)]
38. Park, S.H.; Jin, S.H.; Jun, G.H.; Jeon, S.; Hong, S.H. Enhanced Electrical Properties in Carbon Nanotube/Poly(3-Hexylthiophene) Nanocomposites Formed through Non-covalent Functionalization. *Nano Res.* **2011**, *4*, 1129–1135. [[CrossRef](#)]
39. Park, C.; Ounaies, Z.; Watson, A.K.; Crooks, E.R.; Smith, J.; E Lowther, S.; Connell, J.W.; Siochi, E.J.; Harrison, J.S.; Clair, T.L. Dispersion of Single Wall Carbon Nanotubes by in Situ Polymerization under Sonication. *Chem. Phys. Lett.* **2002**, *364*, 303–308. [[CrossRef](#)]
40. Li, J.; Song, Z.; Gao, L.; Shan, H. Preparation of Carbon Nanotubes/Poly(lactic Acid) Nanocomposites Using a Non-Covalent Method. *Polym. Bull.* **2016**, *73*, 2121–2128. [[CrossRef](#)]
41. Hsiao, A.-E.; Tsai, S.-Y.; Hsu, M.-W.; Chang, S.-J. Decoration of Multi-Walled Carbon Nanotubes by Polymer Wrapping and Its Application in MWCNT/Polyethylene Composites. *Nanoscale Res. Lett.* **2012**, *7*, 240. [[CrossRef](#)]
42. Guo, B.; Ma, P.X. Conducting Polymers for Tissue Engineering. *Biomacromolecules* **2018**, *19*, 1764–1782. [[CrossRef](#)]
43. Hong, J.; Han, J.Y.; Yoon, H.; Joo, P.; Lee, T.; Seo, E.; Char, K.; Kim, B.-S. Carbon-Based Layer-by-Layer Nanostructures: From Films to Hollow Capsules. *Nanoscale* **2011**, *3*, 4515–4531. [[CrossRef](#)]
44. Chen, W.; Liu, P.; Min, L.; Zhou, Y.; Liu, Y.; Wang, Q.; Duan, W. Non-covalently Functionalized Graphene Oxide-Based Coating to Enhance Thermal Stability and Flame Retardancy of PVA Film. *Nano-Micro Lett.* **2018**, *10*, 1–13. [[CrossRef](#)] [[PubMed](#)]
45. Cheng, K.; Li, H.; Zhu, M.; Qiu, H.; Yang, J. In Situ Polymerization of Graphene-Polyaniline@polyimide Composite Films with High EMI Shielding and Electrical Properties. *RSC Adv.* **2020**, *10*, 2368–2377. [[CrossRef](#)]
46. Tian, J.; Xu, T.; Tan, Y.; Zhang, Z.; Tang, B.; Sun, Z. Effects of Non-Covalent Functionalized Graphene Oxide with Hyperbranched Polyesters on Mechanical Properties and Mechanism of Epoxy Composites. *Materials* **2019**, *12*, 3103. [[CrossRef](#)] [[PubMed](#)]
47. Zhang, L.; Wu, H.; Zheng, Z.; He, H.; Wei, M.; Huang, X. Fabrication of Graphene Oxide/Multi-Walled Carbon Nanotube/Urushiol Formaldehyde Polymer Composite Coatings and Evaluation of Their PhysiCo-Mechanical Properties and Corrosion Resistance. *Prog. Org. Coatings* **2019**, *127*, 131–139. [[CrossRef](#)]

48. Palaznik, O.M.; Nedorezova, P.M.; Pol'Shchikov, S.V.; Klyamkina, A.N.; Shevchenko, V.G.; Krashenninnikov, V.G.; Monakhova, T.V.; Arbuzov, A.A. Production by In Situ Polymerization and Properties of Composite Materials Based on Polypropylene and Hybrid Carbon Nanofillers. *Polym. Sci. Ser. B* **2019**, *61*, 200–214. [[CrossRef](#)]
49. Suckeveriene, R.; Tzur, A.; Narkis, M.; Siegmann, A. Grafting of Polystyrene Chains on Surfaces of Nanosilica Particles via Peroxide Bulk Polymerization. *Polym. Compos.* **2009**, *30*, 422–428. [[CrossRef](#)]
50. Rosen-Kligvasser, J.; Suckeveriene, R.Y.; Tchoudakov, R.; Narkis, M. a Novel Methodology for Controlled Migration of Antifog from Thin Polyolefin Films. *Polym. Eng. Sci.* **2013**, *54*, 2023–2028. [[CrossRef](#)]

Publisher's Note: MDPI stays neutral with regard to jurisdictional claims in published maps and institutional affiliations.



© 2020 by the authors. Licensee MDPI, Basel, Switzerland. This article is an open access article distributed under the terms and conditions of the Creative Commons Attribution (CC BY) license (<http://creativecommons.org/licenses/by/4.0/>).